PHYSICAL REVIEW B **74**, 220511(R) (2006)

Collapse of the critical state in superconducting niobium

Ruslan Prozorov,[1,*] Daniel V. Shantsev,[2,3] and Roman G. Mints[4]
[1]*Ames Laboratory and Department of Physics & Astronomy, Iowa State University, Ames, Iowa 50011, USA*
[2]*Department of Physics, University of Oslo, P. O. Box 1048 Blindern, 0316 Oslo, Norway*
[3]*A. F. Ioffe Physico-Technical Institute, Polytekhnicheskaya 26, St. Petersburg 194021, Russia*
[4]*School of Physics and Astronomy, Raymond and Beverly Sackler Faculty of Exact Sciences, Tel Aviv University, Tel Aviv 69978, Israel*

(Received 25 October 2006; published 20 December 2006)

Giant abrupt changes in the magnetic-flux distribution in niobium foils were studied by using magneto-optical visualization, thermal, and magnetic measurements. Uniform flux jumps and sometimes almost total catastrophic collapse of the critical state are reported. Results are discussed in terms of thermomagnetic instability mechanism with different development scenarios.

DOI: 10.1103/PhysRevB.74.220511 PACS number(s): 74.25.Ha, 74.25.Op, 74.25.Qt

Large jumps in magnetization, temperature, ultrasonic attenuation, and resistivity have been observed in many superconducting materials since the early 1960s.[1–6] Although no definitive mechanism has been identified, it is believed that such changes are caused by sudden redistribution of Abrikosov vortices triggered and supported by thermomagnetic instabilities.[1–3,7–12] Direct observations of flux jumps using miniature Hall probes[13–16] and real-time magneto-optical imaging[3,17–21] have confirmed precipitous propagation of flux into the specimen. Although some evidence of large-scale jumps exists,[5,13] direct observations of avalanchelike behavior in films have mostly found dendritic and branched fingerlike patterns (on a macroscopic scale of the whole sample) or small jumps (few tens of micrometers) forming feather-shaped flux fronts.[3,14,15,18–21]

Dendritic avalanches are expected for thin films with high critical current density.[7,11,12] The problem is that dendritic avalanches are too small to result in the observed jumps of magnetization M. If δM is a variation of magnetization during a flux jump, then the dendritic avalanches contribute $\delta M \lesssim 0.1M$.[19] However, the observed changes are often much larger[16,22] (also see Fig. 1). They must be associated with more dramatic catastrophic changes of the critical state when a nonuniform (Bean's) distribution of vortices suddenly collapses. In this paper we present direct observations of the catastrophic collapse of the critical state in niobium foils and provide evidence for thermomagnetic origin of this effect.

Pure Nb (99.99%) strips of various thickness (5, 10, and 25 μm) were obtained from Goodfellow. Sample widths varied from 0.7 to 4 mm and the lengths varied from 2 to 10 mm. Magnetization loops $M(H)$ were measured in a Quantum Design MPMS. Resistivity, specific heat, and transport critical current were measured in a Quantum Design PPMS. We also measured sample temperature variation in quasiadiabatic conditions and found temperature jumps associated with the flux jumps.

Figure 1 shows $M(H)$ in a 25-μm-thick Nb foil at different temperatures, (a) 1.8 K, (b) 3 K, and (c) 4 K. At the lowest temperature, Fig. 1(a), jumps in $M(H)$ are observed both upon penetration after zero-field cooling (ZFC) and upon flux exit. At higher temperatures, jumps were only observed upon reduction of the magnetic field (b), and no jumps were observed above 4 K (c). In Figs. 1(b) and 1(c) curves are shown after the external field was reduced from 5 kOe to zero and an attempt was made to observe jumps upon increasing the magnetic field of the same orientation. Unlike the case of the opposite field, no jumps in $M(H)$ were observed. These results hint at thermomagnetic instability mechanism.[1,2] For comparison of flux jumping instability scenarios in thin foils and bulk samples a large Nb single crystal (5 mm diameter, 1 mm thickness) was measured at several temperatures. Figure 1(d) shows $M(H)$ at $T=4.5$ K for both ascending and descending branches. For other temperatures only descending branches are plotted. Giant magnetization jumps were observed upon decrease of the magnetic field at temperatures up to 5.5 K. Evidently, variation of magnetization at a jump is much larger in a thick sample.

Visualization of the magnetic induction $B(r)$ on the sample surface was performed in a flow-type ^{4}He cryostat with the sample in vacuum attached to a copper heat exchanger (i.e., cooling conditions are different from measurements in Quantum Design MPMS, Fig. 1). Bismuth-doped iron-garnet heterostructure film with in-plane magnetization

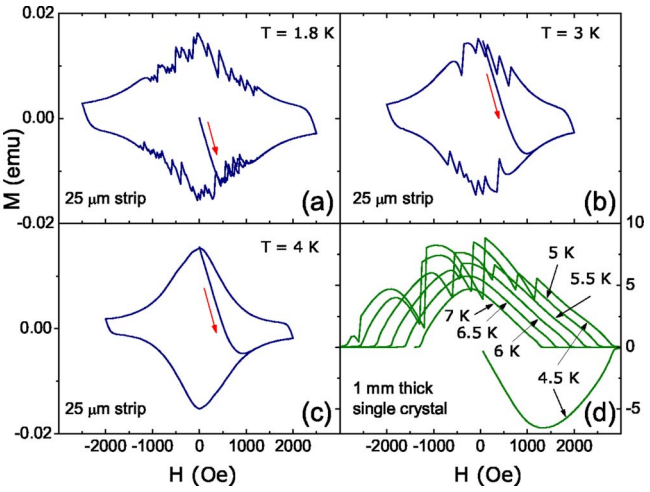

FIG. 1. (Color online) Magnetization loops measured in 25-μm-Nb foil at different temperatures, (a) 1.8 K, (b) 3 K, (c) 4 K, and, for comparison, (d) several M (H) curves measured from 4 to −4 kOe in large Nb single crystal. For (b) and (c) curves start from remanent magnetization, see text for details.

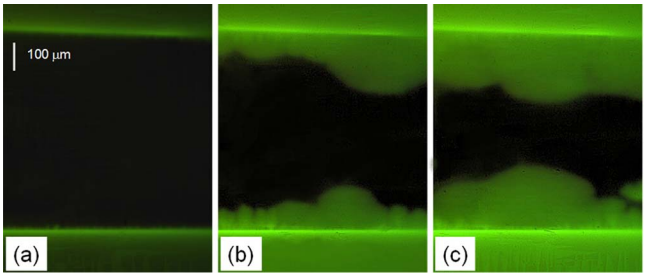

FIG. 2. (Color online) Penetration of magnetic field in 10-μm-thick Nb strip after zero-field cooling. (a) 160, (b) 415, (c) 480 Oe. Penetration in (b) and (c) was avalanchelike at fields indicated. (Real-time video online, Ref. 25.)

was used as a magneto-optical indicator.[23,24] In all images, intensity is proportional to the magnitude of $B(r)$. Moreover, due to the dispersion of the Faraday rotation for different wavelengths, up and down directions of the magnetic induction can be distinguished. In our case, green corresponds to flux out of page and yellow corresponds to the opposite orientation (antiflux). This information is useful for flux-antiflux annihilation experiments described below.

In magneto-optical experiments, sudden collapses of magnetization were observed only below $T \simeq 4.5$ K for all samples. Figure 2 shows penetration of the flux into a 10-μm Nb strip at increasing magnetic fields, (a) 160 Oe, (b) 415 Oe, and (c) 480 Oe. The large-scale abrupt jumps in Figs. 2(b) and 2(c) occurred right before fields at which images were acquired (about 405 and 470 Oe, respectively). In our case of the 30-Hz data acquisition rate, the jumps seem instantaneous. Real-time dynamics can be viewed online.[25]

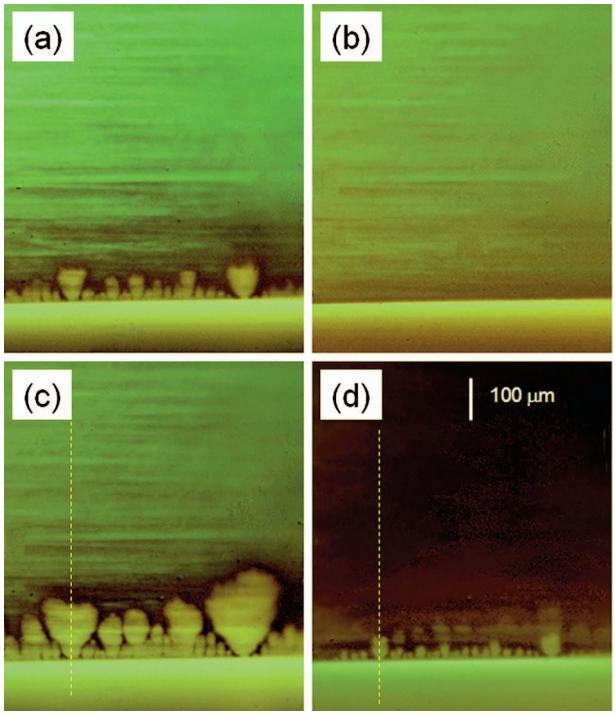

FIG. 3. (Color) Catastrophic collapse of the critical state upon entry of negative self-field at $T=3.9$ K. (a) 250 Oe, (b) 200 Oe, (c) 100 Oe, (d) 50 Oe. (Real-time video online, Ref. 25.)

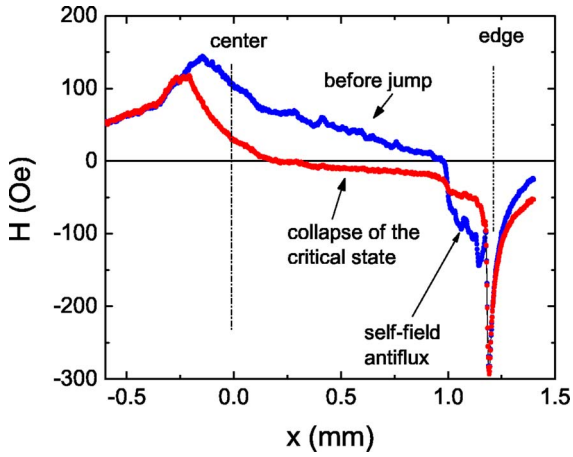

FIG. 4. (Color online) Profiles of the magnetic flux before and after collapse of the critical state upon entry of the negative flux generated by self-field. The profiles were measured along dashed lines in Figs. 3(c) and 3(d).

The largest and most dramatic features occur upon decrease of a magnetic field when self-field antiflux induced at the edges due to large demagnetization factor starts entering the sample. The antiflux annihilates with the trapped flux providing an additional mechanism to trigger thermal instability. An avalanche in progress is difficult to stop, because the whole sample is in the critical state and an increase of temperature leads to reduction of the local critical current density resulting in further flux redistribution. This results in large uniform avalanches when the whole critical state literally collapses. In Fig. 3 two such collapses are shown—panels (b) [jumped after (a)], and (d) [jumped after (c)]. Some intensity banding in Fig. 3 reflects the structure of the trapped flux in this sample.

Flux profiles corresponding to the collapse of the critical state are shown in Fig. 4. The profiles were measured along the dashed lines shown in Figs. 3(c) and 3(d). Clearly, at some magnetic field, the slightest variation results in a change of the entire distribution of vortices. The observed giant jumps may span more than half the width of the

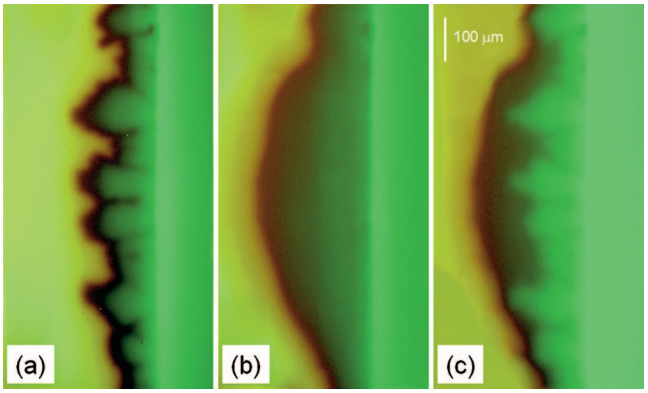

FIG. 5. (Color) Entry of the antiflux (from right to left): (a) −320 Oe, (b) −470 Oe. Note a huge uniform avalanche. (c) −740 Oe. Note secondary penetration on top of the flux distribution flattened by the avalanche. It indicates that j_c returned to its large "cold" values. (Real-time video online, Ref. 25.)

sample. Moreover, the collapse washes away both the interior critical state as well as any newly penetrated antiflux at the edges. When the magnetic field of the opposite polarity is applied, antiflux annihilates with the trapped flux similar to the self-field antiflux discussed above. This results in large uniform avalanches as shown in Fig. 5. In general, the largest avalanches and sometimes total collapse of the critical state occurs at small fields upon entry of an antiflux. We think that this is because critical current density is largest and most strongly field dependent at low fields.

Although thermal instability seems to be the most natural scenario, direct evidence for thermal effects is scarce. Temperature jumps were detected in Nb-Zr alloys.[4] MgB_2 films coated with gold showed suppression of the dendritic avalanches.[27] We report direct measurements of the temperature variation associated with flux jumps in Nb foils. In this experiment, the sample was suspended by four wires on a thin sapphire stage normally used for specific-heat measurements in a Quantum Design PPMS. The arrangement allows for direct reading of the sample thermometer in almost adiabatic conditions.

Figure 6 shows field sweeps (all taken from 3 to −3 kOe). Temperature jumps were detected at the same range of temperatures and fields as magnetization measured in the same sample. To emphasize the variation, it was multiplied by a factor of 20. Indeed, local temperature T_a within the "volume" of the avalanche, $V_a \simeq 5\times10^{-4}$ mm^3, reaches very large values of order of T_c.[10] Then the average temperature measured by the calorimeter is given by $\delta T = T_a V_a / V_t$, where the total volume of the sample $V_t \simeq 5\times10^{-2}$ mm^3. This gives $\delta T \simeq 0.01 T_c$ K, in agreement with the direct measurements, Fig. 6.

In general, there are two channels to dissipate the energy of the critical state—dynamic and adiabatic.[1,2,7] The dynamical channel corresponds to the energy removal to a coolant and it is characterized by the dimensionless parameter, $\alpha = \rho j_c^2 d / h(T_c - T_0)$.[1,2,7,11,12] Here j_c is the critical current, $h \simeq 5$ W/cm^2 K is the heat-transfer coefficient, $\rho \simeq 0.5$ $\mu\Omega$ cm is the normal-state resistivity, d is the thickness, and T_0 is the temperature of the coolant. The adiabatic channel corresponds to the energy absorption by the material itself, which is accompanied by an increase of the sample temperature. The threshold parameter for thin samples is given as $\beta = 4dw j_c^2 / [c^2 C_p^v(T_0)(T_c - T_0)]$,[10] where w is the sample half width. Using the results of direct measurements on our foils, $j_c(T) = 1.5\times10^6(1 - T/T_c)$ A/cm^2 and $C_p(T) = 0.25(T/T_c)^3$ J/mol K, we obtain $\alpha \simeq 8$ and $\beta \simeq 15$. Large values of α and β indicate that both channels can take away only an insignificant fraction of the Joule heat, which makes flux jumps inevitable, in full agreement with our experiments.

A flux jump in a thin sample develops into either a dendritic or uniform pattern depending on the ratio of thermal and magnetic diffusivities, $\tau = \kappa / 4\pi\rho C$, where κ is the thermal conductivity.[12] Qualitatively, if τ is very small, the lateral heat diffusion is slow and flux propagates along narrow channels forming a dendritic pattern. For large τ the heat diffusion establishes essentially uniform temperature distribution and a flux jump spreads out uniformly in all directions. The threshold value is given (for $\alpha \gg 1$) as $\tau_c \approx w / 8dn\beta$,[12] where n is the exponent in the current-voltage law, $E \propto j^n$. For $n = 30$ and $\kappa = 10$ W/Km, we find $\tau \simeq 1$, while $\tau_c \simeq 0.03$ indicating that the flux jumps should develop uniformly—as we indeed observe experimentally. To quantitatively validate these estimates we considered development of flux jumps by numerically solving the thermal diffusion and Maxwell equations, $C_p dT/dt = jE - h(T - T_0)/d$ and $dE/dx = -dH/dt$. The sample was assumed to be a thin infinite strip, where all the quantities depend only on the coordinate x across the strip.

Measured (symbols, corresponding to Fig. 2) and calculated profiles (solid lines) of the magnetic induction are shown in Fig. 7. If we omit the Joule term jE, the calculations produce the well-known Bean-model profiles[26] that perfectly fit the experimental profiles before a jump, see the

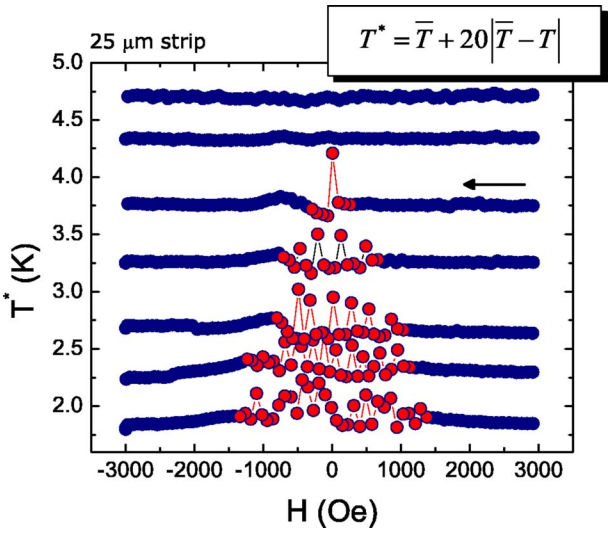

FIG. 6. (Color online) Temperature variation upon decrease of magnetic field from 3 to −3 kOe in a 25-μm-thick Nb foil. The temperature variation was multiplied by a factor of 20 for clear visual appearance.

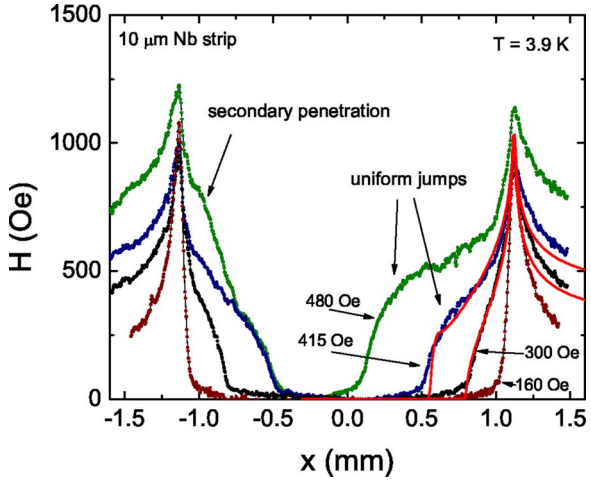

FIG. 7. (Color online) Profiles of magnetic induction in 2.88-mm-wide and 10-μm-thick strip upon flux penetration after ZFC. Two inner profiles correspond to large uniform jumps shown in Fig. 2.

300-Oe curves. If we start from such a Bean profile and, keeping applied field constant, introduce an infinitesimal perturbation in T, a flux jump occurs. The curve for 415 Oe shows the final flux profile after such a jump. Apparently, the agreement with experiment is again very good, which further supports the thermomagnetic mechanism of the observed instability.

Furthermore, we tried to control the rate of heat conductance by introducing a thin mylar film between the heat exchanger and the sample. Both feather-shaped protrusions and large uniform avalanches were observed in this case. Moreover, uniform jumps appeared even in ZFC samples where they were absent before. These experiments demonstrate that reducing the heat link to the thermal bath makes the avalanches more likely to happen.

In conclusion, we observed large scale giant uniform vortex avalanches and even collapse of the critical state in niobium foils. Direct measurements of temperature variation as well as analysis of the magnetic and thermal energy balance support thermomagnetic instability scenario. Comparable values of the magnetic and thermal diffusivities ($\tau \sim 1$) result in spatially uniform giant flux jumps.

We thank Alex Gurevich, Igor Aranson, Yuri Galperin, and Kotane Dam for useful discussions and Thomas A. Girard for providing the samples and for discussions. Ames Laboratory is operated for U.S. DOE by the Iowa State University under Contract No. W-7405-Eng-82. R.P. acknowledges support from NSF Grant No. DMR-05-53285 and from the Alfred P. Sloan Research Foundation.

*Electronic address: prozorov@ameslab.gov

[1] R. G. Mints and A. L. Rakhmanov, Rev. Mod. Phys. **53**, 551 (1981).

[2] A. V. Gurevich, R. G. Mints, and A. L. Rakhmanov, *The Physics of Composite Superconductors* (Begell House Inc., New York, 1997).

[3] E. Altshuler and T. H. Johansen, Rev. Mod. Phys. **76**, 471 (2004).

[4] L. T. Claiborne and N. G. Einspruch, J. Appl. Phys. **37**, 925 (1966).

[5] B. B. Goodman and M. Wertheimer, Phys. Lett. **18**, 236 (1965).

[6] M. Levy, R. Kagiwada, F. Carsey, and I. Rudnick, Phys. Rev. B **2**, 2804 (1970).

[7] I. S. Aranson, A. Gurevich, M. S. Welling, R. J. Wijngaarden, V. K. Vlasko-Vlasov, V. M. Vinokur, and U. Welp, Phys. Rev. Lett. **94**, 037002 (2005).

[8] B. Biehler, B. U. Runge, P. Leiderer, and R. G. Mints, Phys. Rev. B **72**, 024532 (2005).

[9] A. L. Rakhmanov, D. V. Shantsev, Y. M. Galperin, and T. H. Johansen, Phys. Rev. B **70**, 224502 (2004).

[10] D. V. Shantsev, A. V. Bobyl, Y. M. Galperin, T. H. Johansen, and S. I. Lee, Phys. Rev. B **72**, 024541 (2005).

[11] Y. E. Kuzovlev, cond-mat/0607143 (unpublished).

[12] D. V. Denisov, A. L. Rakhmanov, D. V. Shantsev, Y. M. Galperin, and T. H. Johansen, Phys. Rev. B **73**, 014512 (2006).

[13] S. S. James, S. B. Field, J. Seigel, and H. Shtrikman, Physica C **332**, 445 (2000).

[14] E. Altshuler, T. H. Johansen, Y. Paltiel, P. Jin, K. E. Bassler, O. Ramos, Q. Y. Chen, G. F. Reiter, E. Zeldov, and C. W. Chu, Phys. Rev. B **70**, 140505(R) (2004).

[15] P. Esquinazi, A. Setzer, D. Fuchs, Y. Kopelevich, E. Zeldov, and C. Assmann, Phys. Rev. B **60**, 12454 (1999).

[16] V. V. Chabanenko, V. F. Rusakov, S. Piechota, A. Nabialek, S. Vasiliev, and H. Szymczak, Physica C **369**, 82 (2002).

[17] P. Leiderer, J. Boneberg, P. Brull, V. Bujok, and S. Herminghaus, Phys. Rev. Lett. **71**, 2646 (1993).

[18] C. A. Durán, P. L. Gammel, R. E. Miller, and D. J. Bishop, Phys. Rev. B **52**, 75 (1995).

[19] T. H. Johansen, M. Baziljevich, D. V. Shantsev, P. E. Goa, Y. M. Gal'perin, W. N. Kang, H. J. Kim, E. M. Choi, M.-S. Kim, and S. I. Lee, Europhys. Lett. **59**, 599 (2002).

[20] M. S. Welling, R. J. Westerwaal, W. Lohstroh, and R. J. Wijngaarden, Physica C **411**, 11 (2004).

[21] R. J. Wijngaarden, M. S. Welling, C. M. Aegerter, and M. Menghini, Eur. Phys. J. B **50**, 117 (2006).

[22] D. P. Young, M. Moldovan, P. W. Adams, and R. Prozorov, Supercond. Sci. Technol. **18**, 776 (2005).

[23] A. A. Polyanskii, D. M. Feldmann, and D. C. Larbalestier, in *The Handbook on Superconducting Materials*, edited by D. Cardwell and D. Ginley (2003), p. 1551.

[24] C. Jooss, J. Albrecht, H. Kuhn, S. Leonhardt, Kronm, and H. Iler, Rep. Prog. Phys. **65**, 651 (2002).

[25] See EPAPS Document No. E-PRBMDO-74-R10646 for real-time videos. For more information on EPAPS, see http://www.aip.org/pubservs/epaps.html.

[26] E. H. Brandt and M. Indenbom, Phys. Rev. B **48**, 12893 (1993).

[27] Eun-Mi Choi, Hyun-Sook Lee, Hyun Jung Kim, Byeongwon Kang, Sung-Ik Lee, A. A. F. Olsen, D. V. Shantsev, and T. H. Johansen, Appl. Phys. Lett. **87**, 152501 (2005).